Supplementary information

Optimizing Pt Particle Size and Lewis Acidity in Pt/θ-Al_2O_3 Catalysts for Enhanced Perhydro Benzyltoluene Dehydrogenation

Yueqi Wang [a,#], Yu Niu [d,#], Qinglian Wang [a,b,*], Wang Yin [a,b,*], Yixiong Lin [a,b,], Ting Qiu [a,b], Jiafang Gu [c], Chen Yang [a,b,*]

[a] State Key Laboratory of Green and Efficient Development of Phosphor Resources, Fujian University's Engineering Research Center of Reactive Distillation Technology, College of Chemical Engineering, Fuzhou University, Fuzhou, Fujian 350108, China;

[b] Qingyuan Innovation Laboratory, Quanzhou 362801, China;

[c] Fuzhou University Zhicheng College, Fuzhou, Fujian 350108, China;

[d] College of Resources and Chemical Engineering, Sanming University, Sanming 365004, China

[#]These authors are co-first authors of the article.

Corresponding authors: wqlian@fzu.edu.cn (Q. Wang), wangyin@fzu.edu.cn (W. Yin*) &cyang@fzu.edu.cn (C. Yang*)

1 Performance of Pt-based Catalysts Supported on Different Polymorphs of Alumina

1.1 Catalysts Preparation

The γ-Al_2O_3 support was calcined in a muffle furnace under static air at 1050 °C and 1200 °C for 4 hours (heating rate: 2 °C/min) to yield θ-Al_2O_3 and α-Al_2O_3 polymorphs, respectively. Pt-based catalysts with 1 wt% nominal loading were subsequently synthesized on these Al_2O_3 polymorphs (γ, θ, α) via wet impregnation using $(NH_3)_4Pt(NO_3)_2$ as the precursor. The impregnation procedure strictly adhered to the standardized protocol detailed in Section 2.2.1. The resulting catalysts were designated as 1Pt/*x*-Al_2O_3, where *x* denotes the Al_2O_3 crystalline phase (γ, θ, and α).

1.2 Characterization analysis

XRD analysis was performed to characterize the crystalline structure and evaluate changes in Pt particle size. As shown in Fig. S1, γ-Al_2O_3 calcined at 1050 °C exhibited diffraction peaks at 2θ = 32.8°, 36.9°, 39.6°, 45.4°, and 67.3°, corresponding to θ-Al_2O_3 (PDF#47-1771), confirming dominant θ-phase formation.[1] At 1200 °C, distinct peaks emerged at 25.6°, 35.1°, 37.8°, 43.3°, 52.5°, 57.5°, 66.5°, 68.2°, and 76.9°, unambiguously assigned to α-Al_2O_3 (PDF#82-1467) [1]. These results demonstrate controlled phase transformation from γ-Al_2O_3 to θ-Al_2O_3 and α-Al_2O_3 polymorphs via thermal treatment.

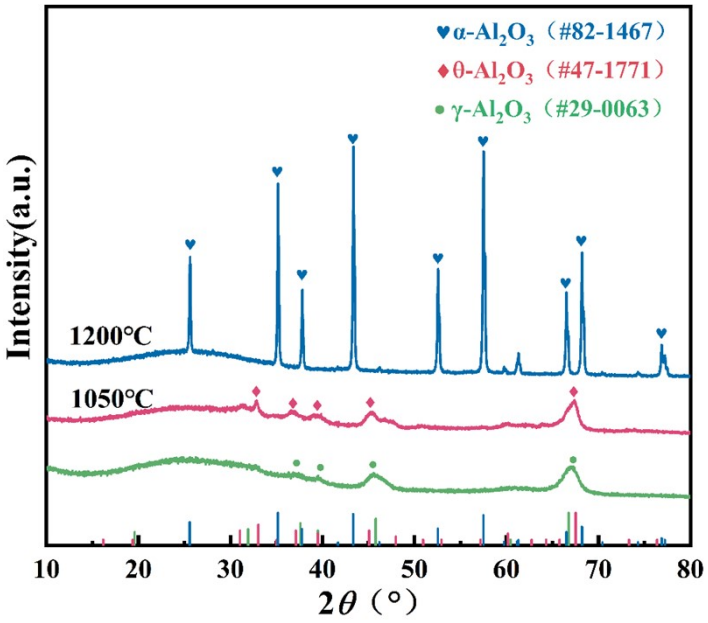

Fig. S1. XRD patterns of *x*-Al_2O_3 catalysts

N_2 adsorption-desorption isotherms and pore size distributions of Al_2O_3 polymorphs (γ, θ, α) are presented in Fig. S2. All phases exhibit Type IV isotherms with H3-type hysteresis loops in the 0.7-1.0 P/P_0 range, confirming characteristic mesoporous structures.[2]

BJH model analysis reveals distinct pore size distributions: γ-Al_2O_3 and θ-Al_2O_3 show narrow distributions peaking at 18 nm and 25 nm, respectively, while α-Al_2O_3 exhibits broad, disordered pore size dispersion. This optimized pore architecture facilitates reactant/product mass transfer and enhances active site accessibility.

As shown in Table. S1, the specific surface area and pore volume of Al_2O_3 were found to decrease significantly with increasing calcination temperature. The specific surface areas of γ-Al_2O_3, θ-Al_2O_3, and α-Al_2O_3 were determined to be 136 m^2/g, 86.7 m^2/g, and 6 m^2/g, respectively, with corresponding pore volumes of 0.82 cm^3/g, 0.62 cm^3/g, and 0.019 cm^3/g. This phenomenon was attributed to pore structure collapse caused by high temperatures. The average pore diameters of the three materials were

measured as 11.9 nm, 21.0 nm, and 6.4 nm, respectively, with larger pore diameters shown to reduce molecular diffusion resistance and accelerate reaction kinetics.

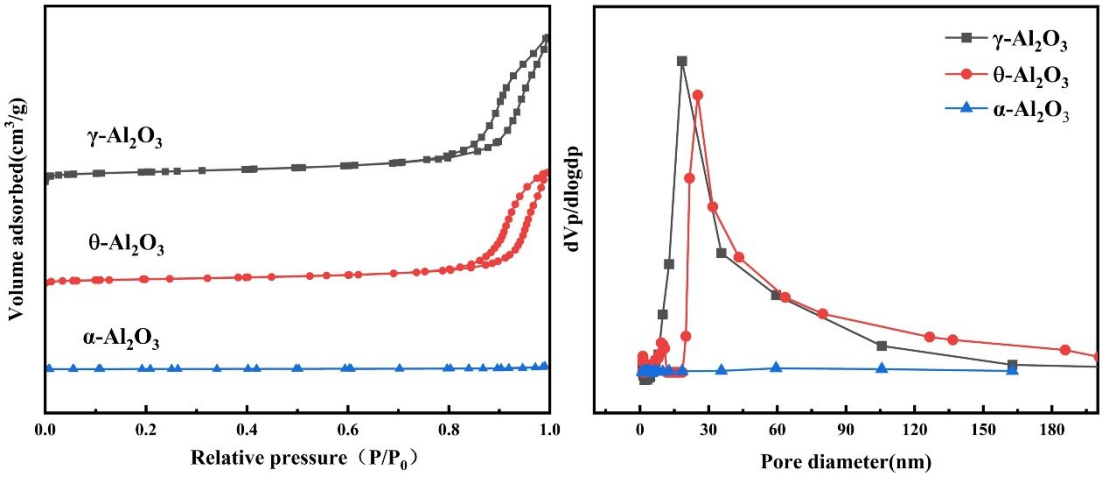

Fig. S2. N_2 adsorption and desorption isotherms and pore size distribution of *x*-Al_2O_3

Table. S1. Specific surface area and pore structure parameters of the material

Samples	BET area (m^2/g)[a]	Pore Size(nm)[b]	Pore Volume(cm^3/g)
γ-Al_2O_3	136.0	11.9	0.82
θ-Al_2O_3	86.7	21.0	0.62
α-Al_2O_3	6.0	6.4	0.019

a, b are derived from BET and BJH methods, respectively.

1.3 Dehydrogenation performance

Under identical reaction conditions (250°C, 0.05 mol% Pt/H12-BT, 300 rpm), the 1Pt/θ-Al_2O_3 catalyst exhibited superior dehydrogenation performance compared to 1Pt/γ-Al_2O_3 and 1Pt/α-Al_2O_3 counterparts, as shown in Fig. S3. This performance hierarchy could be directly attributed to the larger average pore size of θ-Al_2O_3, as indicated in Table. S1. This larger pore size helped reduce the diffusion resistance of reactants and promoted the desorption of products.[3]

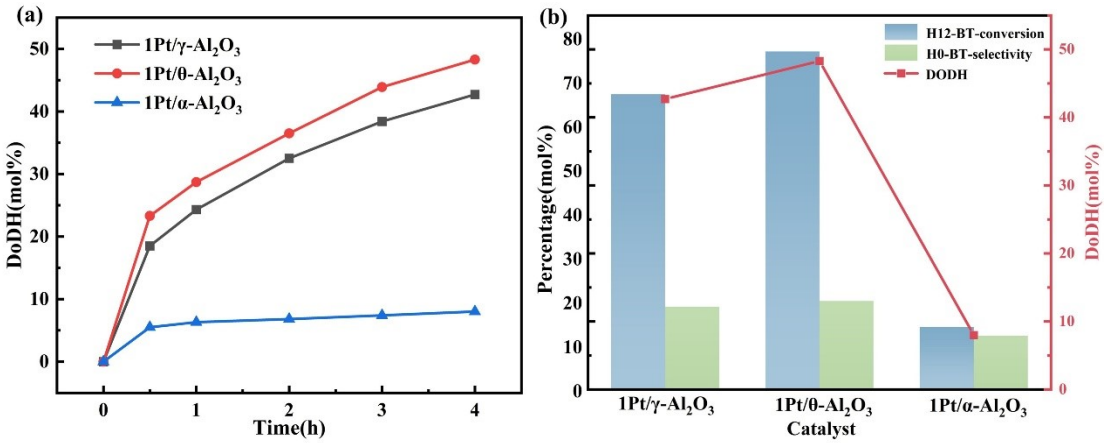

Fig. S3. Dehydrogenation performance of 1Pt/*x*-Al_2O_3 catalysts: (a) Degree of dehydrogenation versus time, (b) Dehydrogenation degree, H12-BT conversion and H0-BT selectivity at 4 h of reaction

2 Catalyst characterization method

Catalyst characterization was performed using the following analytical techniques:

X-ray diffraction (XRD) analysis was conducted on a Rigaku Ultima IV diffractometer with Cu Kα radiation (λ = 1.5406 Å), scanning 2θ from 10° to 80° at 10 °/min with a step size of 0.02°.

N_2 physisorption measurements employed an ASAP 2460 instrument. Samples were degassed at 300°C for 3 h under vacuum before analysis at -196 °C. Specific surface areas were calculated using the Brunauer-Emmett-Teller (BET) method, while pore size distributions were derived from the Barrett-Joyner-Halenda (BJH) model applied to the adsorption branch.

Inductively Coupled Plasma Optical Emission Spectrometry (ICP-OES) was performed using an Agilent 7800 spectrometer (Agilent Technologies, USA) to determine metal loadings.

CO chemisorption was conducted on a BELCAT II analyzer. Approximately 0.10

g of catalyst was loaded into a U-shaped quartz reactor, reduced in situ, and subjected to pulsed 5% CO/He injections at constant temperature. Metal dispersion and particle size were calculated from chemisorbed CO quantities monitored by thermal conductivity detection (TCD).

Transmission electron microscopy was performed on a Thermo Scientific Talos F200X G2 operated at 200 kV. High-resolution TEM (HRTEM), high-angle annular dark-field STEM (HAADF-STEM), and energy-dispersive X-ray spectroscopy (EDS) elemental mapping were acquired using an aberration-corrected STEM detector with ultra-large solid angle.

X-ray photoelectron spectroscopy (XPS) measurements utilized a Thermo Scientific K-Alpha spectrometer with monochromatic Al Kα radiation (1486.7 eV) at 72 W (12 kV × 6 mA). Charge correction referenced the C 1s peak at 284.8 eV.

H_2-Temperature Programmed Reduction (H_2-TPR) was employed to investigate the reduction temperature and metal-support interaction. Samples (50 mg) were purged with Ar, then heated to 700°C at 10 °C/min under 10% H_2/Ar flow with TCD monitoring.

H_2-Temperature Programmed Desorption (H_2-TPD) was used to analyze H_2 adsorption behavior on the catalyst surface. Pretreated samples (400 °C, H_2/Ar) were cooled to 50 °C, purged with Ar, then heated to 650°C at 10°C/min under Ar flow.

NH_3-Temperature Programmed Desorption (NH_3-TPD) was utilized to evaluate the catalyst surface acidity and acid distribution. Samples saturated with 5% NH_3/He were purged with He, then heated to 700 °C at 10 °C/min under He flow.

Pyridine-infrared spectroscopy(Py-IR) was performed on a Bruker Tensor 27 spectrometer. Samples were pretreated at 350 °C under vacuum, exposed to pyridine vapor, and spectra were recorded at 150-300 °C after equilibrium.

Thermogravimetric analysis (TGA) used a NETZSCH STA 449 F5 instrument. Samples were heated from ambient temperature to 600 °C at 5 °C/min under N_2 (50 mL/min), with simultaneous recording of TG/DTG curves.

Elemental analysis (CHN) was performed on a German Elementar Unicube elemental analyzer. The samples were dried at 105 °C for 5 h, weighed, and then combusted in a high-purity oxygen atmosphere. The resulting gases (CO_2, H_2O, and N_2/NO_x) were separated and quantified by thermal conductivity detection.

3 Supplementary Tables and Figures

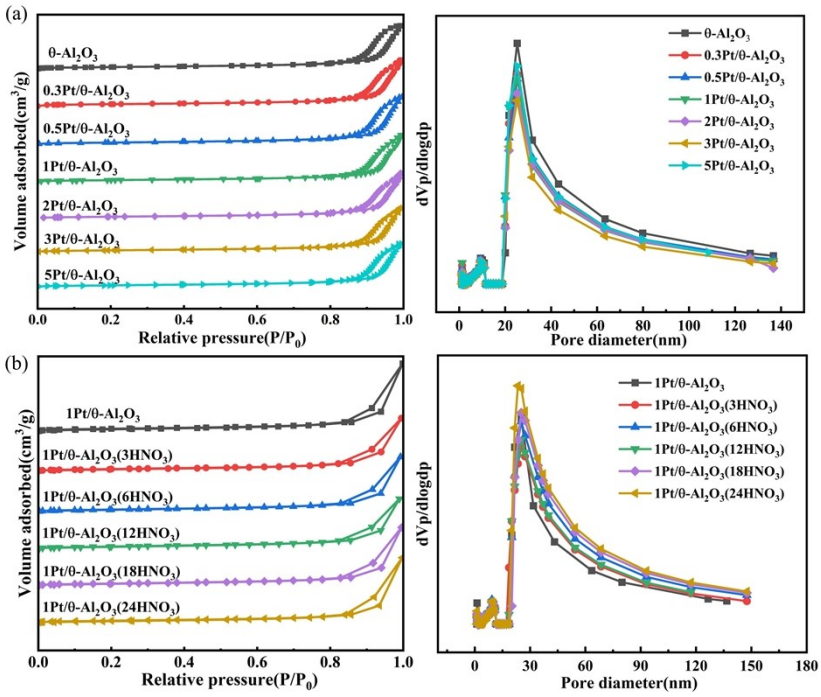

Fig.S4. N_2 adsorption-desorption isotherms and pore size distributions of (a) *y*Pt/θ-Al_2O_3 catalysts; (b) 1Pt/θ-Al_2O_3(*n*HNO_3) catalysts

Table.S2 Chromatographic analysis conditions

Category	Specific Conditions
Column model	Restek RXi®-17Sil MS
Capillary column specifications	30 m×0.25 mm×0.25 μm
Detector temperature	300.0 ℃
Vaporization chamber temperature	300.0 ℃
Pressure	50.2 kPa
Total flow	152.2 mL/min
Column flow	0.5 mL/min
Linear velocity	15.9 cm/sec
Purge flow	3.0 mL/min
Split ratio	300.0
Column temperature	80.0 ℃
Temperature program	Initial temperature 80 °C, ramped to 280 °C at 10 °C/min, held for 2 min

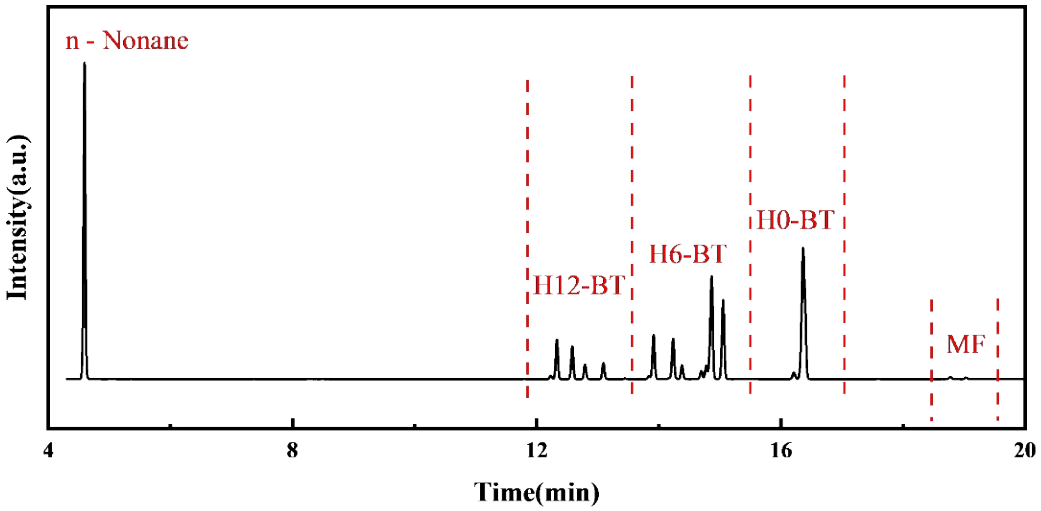

Fig.S5. Chromatographic peaks of H12-BT, H6-BT, and H0-BT

Table.S3. Effects of HNO_3 addition on solution pH and Pt particle size.

Catalyst	HNO_3/Pt molar ratio	pH of the impregnation solution	Pt particle size(nm)
1Pt/θ-Al_2O_3	0	7.5	3.0
1Pt/θ-Al_2O_3(3HNO_3)	3	4.1	3.1
1Pt/θ-Al_2O_3(6HNO_3)	6	2.7	2.9
1Pt/θ-Al_2O_3(12HNO_3)	12	2	2.4
1Pt/θ-Al_2O_3(18HNO_3)	18	1.8	2.4
1Pt/θ-Al_2O_3(24HNO_3)	24	1.6	2.4

Note:The point of zero charge (PZC) of the Al_2O_3 support is 8-9.[4]

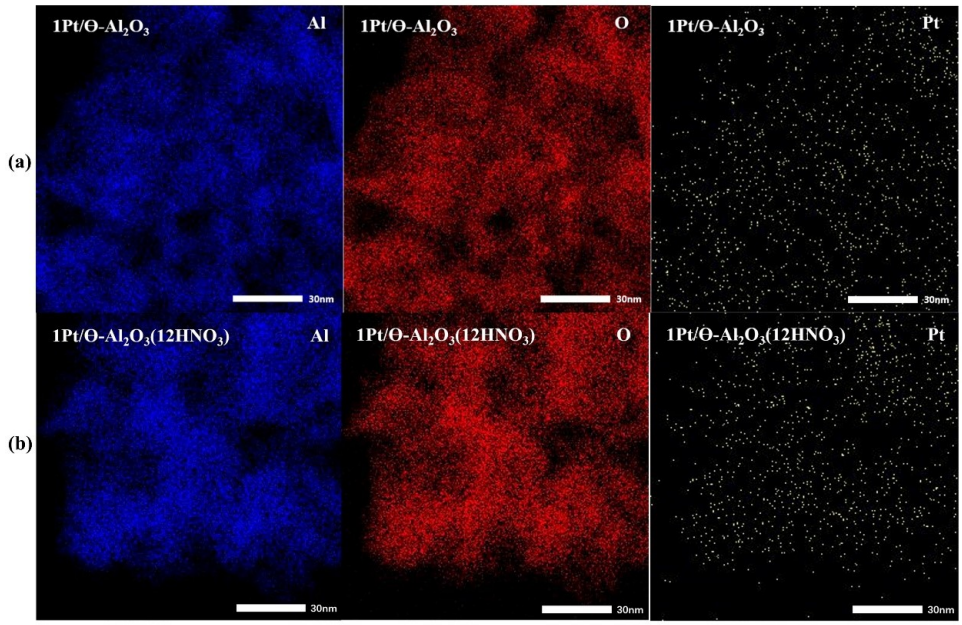

Fig.S6. EDS mapping of (a) 1Pt/θ-Al_2O_3 catalyst (b) 1Pt/θ-Al_2O_3(12HNO_3) catalyst.

Table. S4. Binding energy of Pt 4d orbit of *y*Pt/θ-Al_2O_3 and 1Pt/θ-Al_2O_3 (*n*HNO_3) catalysts

Samples	Binding Energy (eV)	
	Pt^{2+}	Pt^{0+}
0.5Pt/θ-Al_2O_3	317.9/335.2 (43.4%)	315.1/332.3 (56.6%)
1Pt/θ-Al_2O_3	317.8/335.1 (43.0%)	314.6/331.9 (57.0%)
2Pt/θ-Al_2O_3	317.1/334.4 (37.8%)	314.2/331.5 (62.2%)
3Pt/θ-Al_2O_3	316.9/334.2 (32.7%)	314.1/331.4 (67.3%)
5Pt/θ-Al_2O_3	316.6/333.7 (31.1%)	313.7/330.6 (68.9%)
1Pt/θ-Al_2O_3(3HNO_3)	318.0/335.3 (43.2%)	314.7/332.0 (56.8%)
1Pt/θ-Al_2O_3(12HNO_3)	318.3/335.4 (43.8%)	315.3/332.4 (56.2%)
1Pt/θ-Al_2O_3(24HNO_3)	318.4/335.8 (50.8%)	315.5/332.8 (49.2%)

Table.S5. Nitrogen element analysis of the.1Pt/θ-Al_2O_3 ($n$$HNO_3$) catalysts

Catalyst	N（%）
1Pt/θ-Al_2O_3	< 0.3
1Pt/θ-Al_2O_3(3HNO_3)	< 0.3
1Pt/θ-Al_2O_3(6HNO_3)	< 0.3
1Pt/θ-Al_2O_3(12HNO_3)	< 0.3
1Pt/θ-Al_2O_3(18HNO_3)	< 0.3
1Pt/θ-Al_2O_3(24HNO_3)	< 0.3

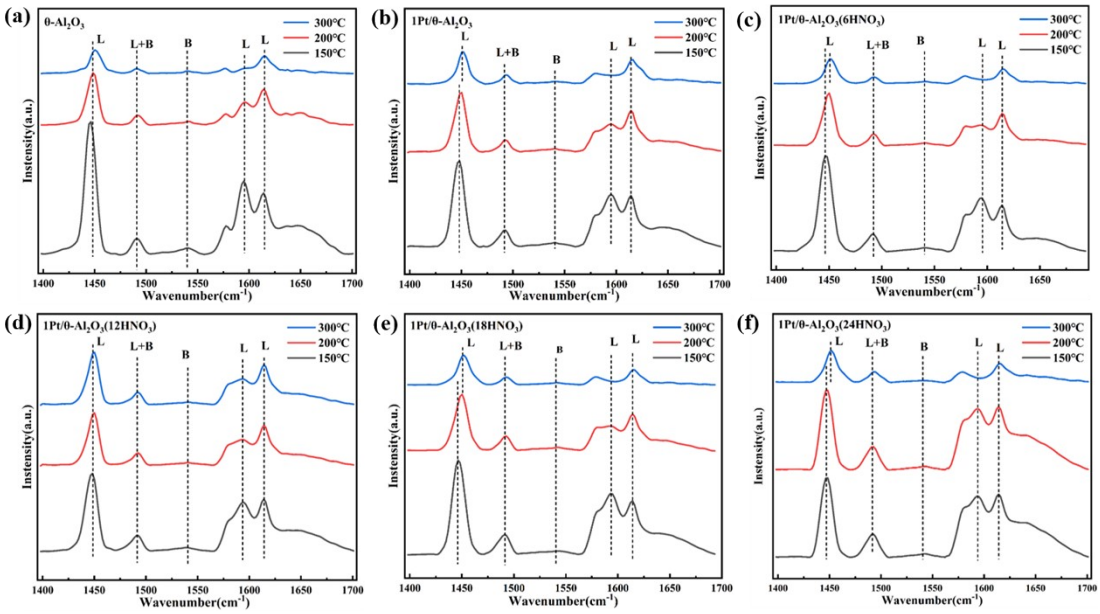

Fig.S7. Py-IR of θ-Al_2O_3 support and 1Pt/θ-Al_2O_3($n$$HNO_3$) catalysts.

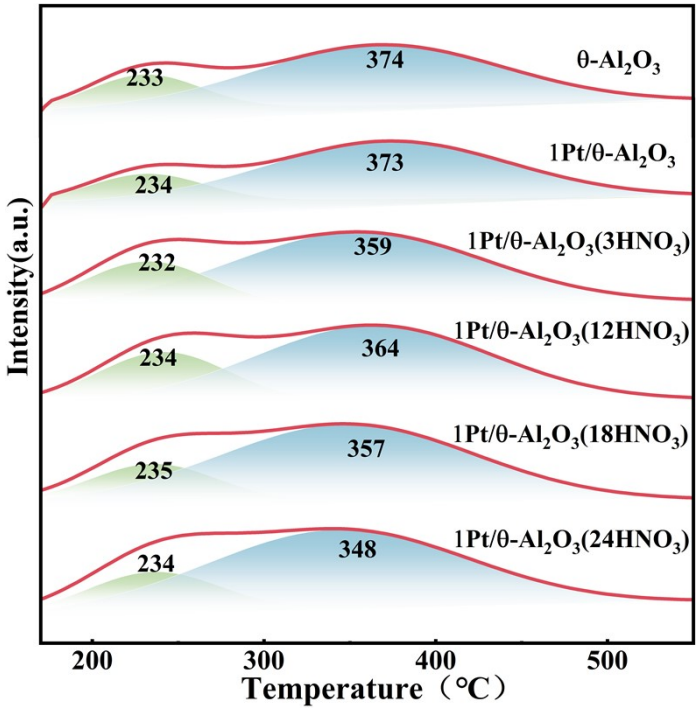

Fig.S8.NH_3-TPD profiles of θ-Al_2O_3 support and 1Pt/θ-Al_2O_3(*n*HNO_3) catalysts.

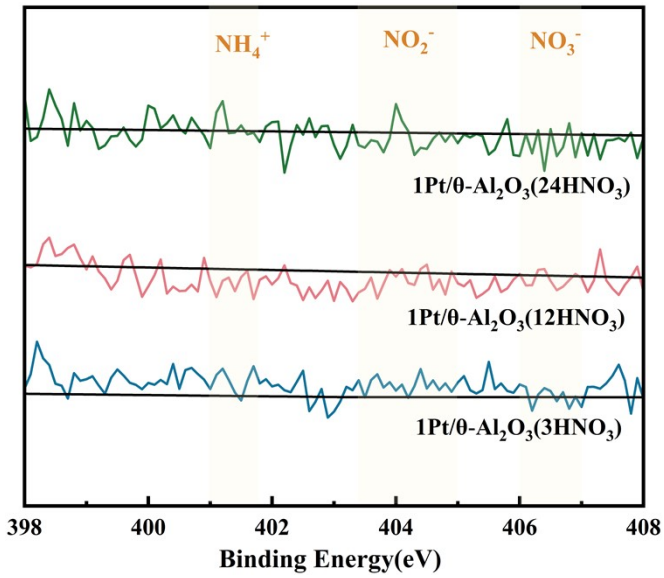

Fig.S9.N 1s XPS spectra of 1Pt/θ-Al_2O_3(*n*HNO_3) catalysts

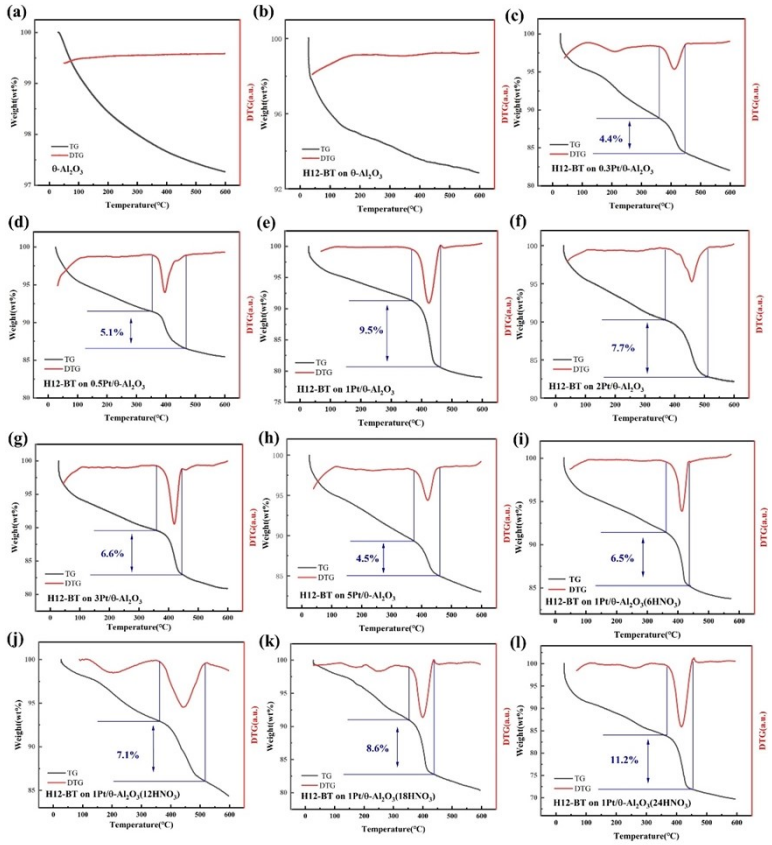

Fig.S10. TG results of H12-BT adsorbed samples:(a) θ-Al_2O_3; (b) H12-BT on θ-Al_2O_3; (c) H12-BT on 0.3Pt/θ-Al_2O_3; (d) H12-BT on 0.5Pt/θ-Al_2O_3; (e) H12-BT on 1Pt/θ-Al_2O_3; (f) H12-BT on 2Pt/θ-Al_2O_3; (g) H12-BT on 3Pt/θ-Al_2O_3; (h) H12-BT on 5Pt/θ-Al_2O_3; (i) H12-BT on 1Pt/θ-Al_2O_3(6HNO_3); (j) H12-BT on 1Pt/θ-Al_2O_3(12HNO_3); (k) H12-BT on 1Pt/θ-Al_2O_3(18HNO_3); (l) H12-BT on 1Pt/θ-Al_2O_3(24HNO_3).

4. H12-BT Dehydrogenation

To establish optimal reaction conditions for H12-BT dehydrogenation, single-factor experiments systematically evaluated stirring speed, temperature, and catalyst dosage.

4.1 Effect of Stirring Speed

Under standardized reaction conditions (250 °C, 4 h, 5 g of H12-BT substrate, 0.05 mol% Pt loading on H12-BT), the dehydrogenation performance of 1Pt/θ-Al_2O_3 and

1Pt/θ-Al_2O_3(12HNO_3) catalysts was systematically evaluated over a stirring rate range of 0-300 rpm. As depicted in Fig. S7, increasing the stirring speed from 0 rpm to 200 rpm results in a marked enhancement in the degree of dehydrogenation (DoDH) over both catalysts, with DoDH values reaching 46.5% and 56.4% for 1Pt/θ-Al_2O_3 and 1Pt/θ-Al_2O_3(12HNO_3), respectively. This phenomenon can be primarily ascribed to the alleviation of external diffusion limitations and the concomitant improvement in interfacial mass transfer efficiency. When the stirring speed is further elevated to 300 rpm, negligible variations can be observed in the DoDH, H12-BT conversion, and H0-BT selectivity over the two catalysts, with DoDH values marginally increasing to 48.3% and 58.7%, respectively. At this stirring rate, the external mass transfer resistance is essentially eliminated, such that the overall reaction rate becomes dominated by internal mass transfer within the catalyst matrix and/or intrinsic reaction kinetics. Although the catalytic activity gain at 300 rpm relative to 200 rpm is modest, operation at 300 rpm confers a certain degree of operational flexibility to the reaction system. Consequently, 300 rpm is designated as the optimal stirring speed for subsequent experiments.

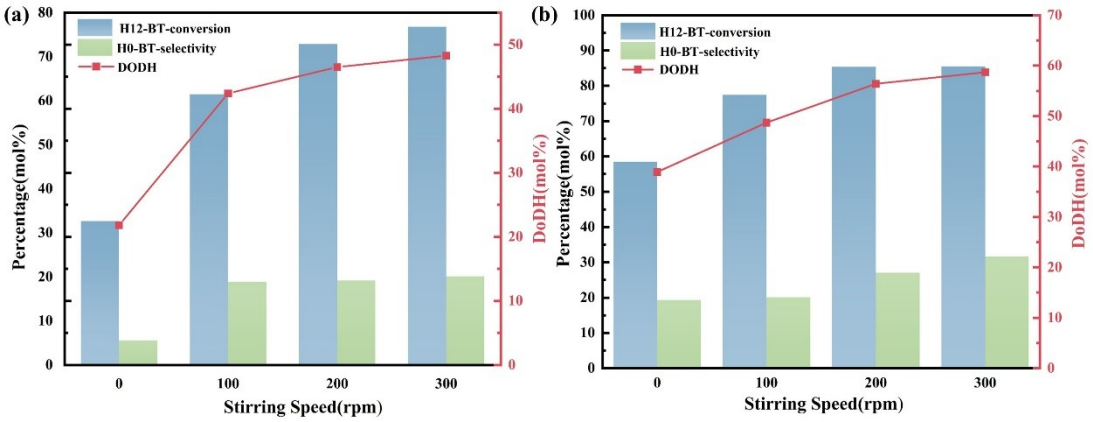

Fig.S11.Stirring speed effect on H12-BT dehydrogenation activity. (a) 1Pt/θ-Al_2O_3 catalyst (b) 1Pt/θ-Al_2O_3(12HNO_3) catalyst. (reaction conditions: 250 °C, 4 h, 5 g H12-BT, 0.05 mol%

catalyst).

4.2 Effect of Reaction Temperature

The impact of temperature on catalytic dehydrogenation performance was systematically investigated over a temperature range of 240, 245, 250, and 255 °C, with the corresponding results illustrated in Fig. S8. As the temperature is gradually elevated from 240 °C to 250 °C, DoDH, H12-BT conversion, and H0-BT selectivity over the 1Pt/θ-Al_2O_3 and 1Pt/θ-Al_2O_3(12HNO_3) catalysts are enhanced to 48.3%, 76.8%, 20.1% and 58.7%, 85.5%, 31.7%, respectively. This performance enhancement can be attributed to the intensified activation of H12-BT reactant molecules at elevated temperatures. When the temperature is further increased to 255 °C, the DoDH values of the two catalysts exhibit only marginal increments of 0.4% and 0.2%, respectively. In consideration of the limited activity gain at 255 °C as well as the elevated energy consumption associated with higher reaction temperatures, 250 °C is identified as the optimal reaction temperature for subsequent experimental investigations.

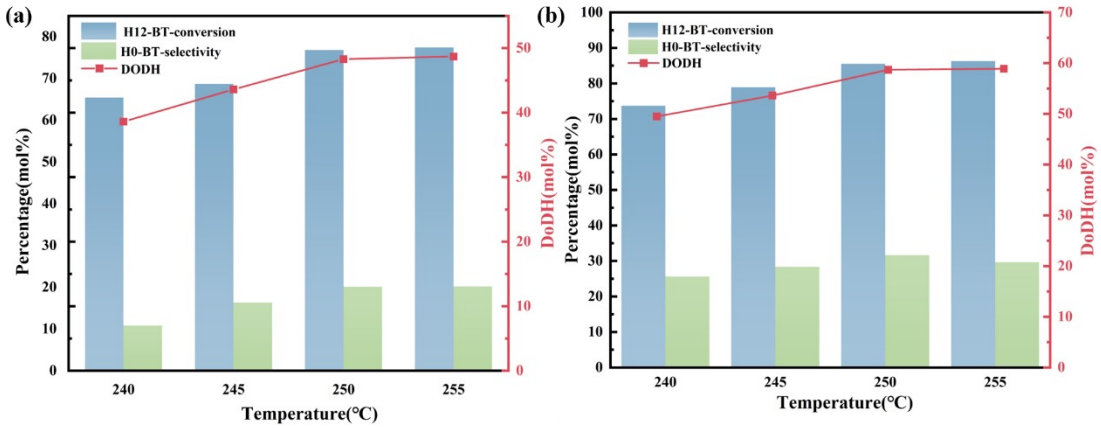

Fig.S12. Reaction temperature effect on H12-BT dehydrogenation activity. (a) 1Pt/θ-Al_2O_3 catalyst (b) 1Pt/θ-Al_2O_3(12HNO_3) catalyst. (reaction conditions: 4 h, 5 g H12-BT, 0.05 mol% catalyst, 300 rpm);

4.3 Effect of Catalyst Dosage

The influence of varying Pt loadings (0.01, 0.03, 0.05, and 0.1 mol%) on the dehydrogenation performance of the reaction system was systematically investigated. The corresponding results are depicted in Fig. S9. As the Pt loading increases from 0.01 mol% to 0.05 mol%, DoDH, H12-BT conversion, and H0-BT selectivity over both 1Pt/θ-Al_2O_3 and 1Pt/θ-Al_2O_3(12HNO_3) catalysts are significantly enhanced. This improvement is primarily ascribed to the increased number of accessible active sites afforded by the higher Pt loading. However, when the Pt loading is further elevated to 0.1 mol%, the enhancement in catalytic performance becomes marginal. This observation indicates that the active sites approached saturation at this loading level; further increasing the Pt loading contributed minimally to improving reaction efficiency, while potentially leading to increased costs and the emergence of mass-transfer limitations. Based on the aforementioned analysis, 0.05 mol% is identified as the optimal Pt loading for the dehydrogenation reaction.

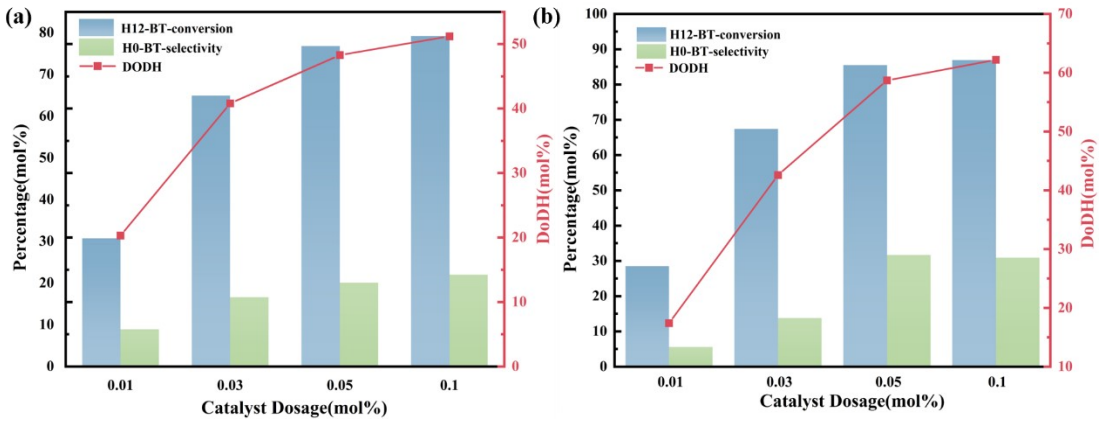

Fig.S13. Catalyst dosage effect on H12-BT dehydrogenation activity. (a) 1Pt/θ-Al_2O_3 catalyst (b) 1Pt/θ-Al_2O_3(12HNO_3) catalyst. (reaction conditions: 250 °C, 4 h, 5 g H12-BT, 300 rpm)

In summary, the optimized reaction conditions for H12-BT dehydrogenation over

both catalysts are determined as follows: stirring speed of 300 rpm, reaction temperature of 250 °C, catalyst loading of 0.05 mol%, reaction time of 4 h, and H12-BT amount of 5 g.

References

1 X. Wang, J. Fan, Z. Zhao, Z. Chen, P. Zheng, J. Li, Y. Li, L. Han, A. Duan, C. Xu, *Energy Fuel*, 2017, **31**, 7456-7463.

2 G. Jiang, L. Jin, Q. Pan, N. Peng, Y. Meng, L. Huang, H. Wang, *Environ. Technol.*, 2021, **43**, 3248-3261.

3 M. Kot, R. Wojcieszak, E. Janiszewska, M. Pietrowski, M. Zieliński, *Materials*, 2021, **14**, 968.

4 G.A. Parks, *Chem. Rev.*, 1965, **65**, 177-198.